Obstacle Avoidance Strategy of Mobile Robot Based on Improved Artificial Potential Field Method

Wei Zhang, Guojun Xu*, Yan Song, Yagang Wang

[a]*Shanghai Key Lab of Modern Optical System and Engineering Research Center of Optical Instrument and System Ministry of Education, School of Optical-Electrical and Computer Engineering, University of Shanghai for Science and Technology, Shanghai, 200093, China.*

Abstract

When there are obstacles around the target point, the mobile robot cannot reach the target using traditional Artificial Potential Field (APF). Besides, the traditional APF is prone to local oscillation in complex terrain such as three-point collinear or semi-closed obstacles. Aiming at solving the defects of traditional APF, a novel improved APF algorithm named back virtual obstacle setting strategy-APF (BVO-APF) has been proposed in this paper. There are two main advantages of the proposed method. Firstly, by redefining the gravitational function as logarithmic function, the proposed method can make the mobile robot reach the target point when there are obstacles around the target. Secondly, the proposed method can avoid falling into local oscillation for both three-point collinear and semi-closed obstacles. Compare with APF and other improved APF, the feasibility of the algorithm is proved through software simulation and practical application.

Keywords: `mobile robot , Artificial Potential Field Method ,Back Virtual Obstacle Setting Strategy , local oscillation`

1. Introduction

With the rapid development of artificial intelligence, mobile robots are widely used in various fields such as medical, industrial and military. For mobile robots, the path planning algorithm is equivalent to the eyes of the robot and plays a crucial role. How the robot chooses a safe and collision-free optimal path from the initial point to the target point is the research focus of the path planning algorithm. Commonly used algorithms are A* algorithm, Ant Colony Optimization, ACO, Genetic Algorithm, GA, Dijkstra algorithm[16][26][23][27][30], Rapidly-Exploring Random Tree, RRT, Artificial Potential Field, APF[13], etc. The A* algorithm[11]introduces a heuristic function to avoid a large number of invalid search paths in the path planning problem. ACO is a heuristic random search algorithm, which has problems such as large amount of calculation and slow convergence. The main characteristics of the Dijkstra algorithm[7] are the center spreads outward until it reaches the end point,

*Corresponding Author
Email address: `747672336@qq.com` (Guojun Xu)

but it traverses many computing nodes, and the efficiency is low. The path obtained by GA meets the actual path selection requirements, but the calculation amount is large and the time consuming is big, which cannot meet the real-time requirements. The main feature of RRT[29][16]is that it generates a new node in space and continues to extend to the target point on the new node, but the generated path is not smooth enough, and the searched path is constantly changing. Bio-inspired algorithms[10][22][4][1][15], can yield good solutions, but they are not necessarily the best solution. All the mentioned algorithms have their respective advantages and disadvantages. In the APF method, you only need to know the current position of the mobile robot, the surrounding obstacles and the position of the target to be reached, and then you can know the moving position of the next part of the robot. It has the advantages of fast speed and smooth generated road strength, so the algorithm is widely used in the path planning of mobile robots. However, the APF method also has its own shortcomings. Firstly, it is easy to fall into local oscillation in complex terrain. Secondly, the robot often fails to reach the target point when there are obstacles near the target point. When the target point is far away, it is easy to collide with obstacles due to the excessive gravitational force generated. By adding a force based on the tangent line between the robot and the obstacle, Wang et al[25] [17] enabled the robot to escape when trapped in a local oscillation. But in the face of semi-closed obstacles, the robot cannot escape the local oscillation. Wang and Lee D et al[8][18] set a virtual target point to make the robot escape from the local oscillation point by setting a virtual target point to provide gravity when the robot falls into local oscillation. Rostami[21] added adjustment factors to the traditional artificial potential field function to bypass obstacles to overcome local minima and target unreachable problems. However, in the face of special semi-closed obstacles, there is no way to set virtual target points. He et al[2] redefined the repulsion model of artificial potential field method by simulating the fading algorithm, and designed a controller that can escape local oscillation. The global path is smooth, but it still cannot be well solved in the face of complex path conditions. Xu et al[28] proposed an improved artificial potential field method. Firstly, the concept of safe distance was proposed to avoid unnecessary paths, so as to solve the problems of long path length and long algorithm running time. Then, in order to avoid the robot being trapped in the local minimum and trap area, the predictive distance was introduced into the algorithm, so that the algorithm was able to react before the robot being trapped in the local minimum or trap area. Finally, the robot was guided to avoid the local minimum and trap area by setting the virtual target points reasonably. Chen and Huang[3]described the inherent problems of artificial potential field and analyzes their causes. Then, aiming at the problem of local minimum trap, the virtual obstacle method is proposed to repel mobile robot from traps. Next, in order to solve the chattering phenomenon, a geometric method is proposed to ensure that the route is relatively smooth. Finally, computer simulations are carried out to demonstrate the effec-

tiveness of these two methods. Neurofuzzy systems[14][24] are also the algorithms that have served as the core methodology to develop path planning. It simulated the workspace of the robot as a network of neurons. Fan and Guo[9]proposed the regular hexagon bootstrap method to improve the local minima problem. At the same time, a relative velocity method for moving object detection and avoidance is proposed for dynamic environment. However, when the obstacle suddenly accelerates or changes its direction of motion, it may cause collision. Montiel et al[20] introduced a parallel evolutionary APF for the dynamic environment. It can achieve controllability in complex real-world sceneries with dynamic obstacles. Cheng et al[5] proposed a novel integrated AUV path planning algorithm by combining the velocity synthesis and APF. Zheng and Edwin [12] proposed a new algorithm based on an artificial potential field and hierarchical cell decomposition technique is developed to solve the find-path problem for a mobile robot. Liu and Zhao[19] proposed an improved particle swarm optimization (IPSO) algorithm, which combines the PSO with the Zigzag algorithm to preplan the search routes and improve the efficiency of the UAVs to search the plume. The improved artificial potential field method is used to avoid dynamic obstacles effectively,and the velocity synthesis algorithm is used to achieve the optimal path.

In view of the problems and deficiencies mentioned above, a novel improved APF algorithm named BVO-APF has been proposed. The main contributions of this paper are concluded as follows.

(1).By redefining the gravitational formula as logarithmic function of traditional APF, the proposed BVO-APF algorithm can reach the target point when there exist obstacles around it. When there are obstacles around the target point, the gravity received by the robot is too small to overcome the repulsion, the robot cannot reach the target point. To solve the above problems, we redefine the gravitational formula of APF. According to the definition of logarithmic function proposed in this paper. When the robot approaches the target point, the gravity obtained by the robot will overcome the repulsion. Eventually the robot will reach the target point.

(2).In the BVO-APF algorithm, tangent algorithm and back virtual obstacle setting strategy are proposed. The robot can avoid falling into local oscillation for both three-point collinear and semi-closed obstacles.

(3).In this paper, the algorithm proposed in this paper is simulated and contrasted through the Matlab software simulation platform and the ROS vehicle simulation platform. The algorithm proposed in this paper has good feasibility and practicability, no matter in simulation experiment or entity demonstration.

2. Basic principle of artificial potential field method

The APF was first proposed by Khatib[13] as a virtual force method. His core idea is to put the robot in the surrounding environment and design it to move in an abstract artificial

gravitational field. There are two types, one is the gravitational force between the robot and the target point, and the other is the repulsive force between the robot and the obstacle. The resultant force provides the driving force for the robot.

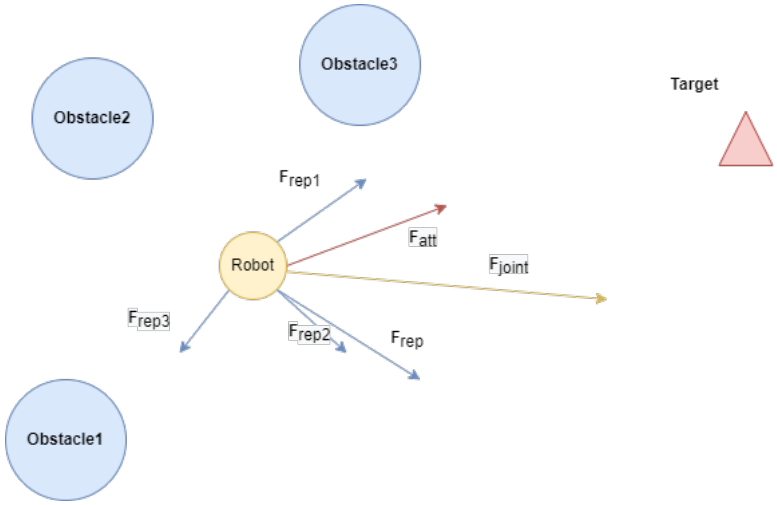

Fig. 1 Schematic diagram of APF

The gravitational force[13] of the robot on the obstacle is U_{att}, the coordinate of the target point is (x_o, y_o),the position of the real-time center point of the robot is (x, y). The APF defines the gravitational function as : $U_{att} = \frac{1}{2} \cdot \varepsilon \rho_o^2$, $\rho_o = \sqrt{(x + x_o)^2 + (y + y_o)^2}$, where ρ_o is the Euclidean length from the center coordinates of the robot to the coordinates of the target point, ε is the gain coefficient of the gravitational potential field.

With the gravitational function, the gravitational force of the APF is the derivative of the gravitational field to the distance. $F_{att} = - \bigtriangledown U_{att} = \varepsilon \rho_o$, where F_{att} represents the gravitational force on the robot. The repulsive field formula U_{rep} F_{rep} are defined as:

$$U_{rep} = \begin{cases} \frac{1}{2}\mu(\frac{1}{\rho_{ob}} - \frac{1}{\rho})^2 & \text{if } \rho_{ob} \leq \rho \\ 0 & \text{if } \rho_{ob} \geq \rho \end{cases} \tag{1}$$

$$F_{rep} = \begin{cases} \mu(\frac{1}{\rho_{ob}} - \frac{1}{\rho}) \cdot \frac{1}{\rho_{ob}^2} & \text{if } \rho_{ob} \leq \rho \\ 0 & \text{if } \rho_{ob} \geq \rho \end{cases} \tag{2}$$

where $\rho_{ob} = \sqrt{(x - x_{ob})^2 + (y - y_{ob})^2}$ represents the distance between the robot and the obstacle. where ρ represents a safe distance between the robot and the obstacle. Outside this distance, the repulsion of the obstacle has no effect on the robot. When it is less than this threshold, the repulsion of the obstacle to the robot is affected by the distance between the two.

When the robot is within the influence range of multiple obstacles, its repulsive force is the sum of multiple repulsive forces ,the resultant force of the repulsive force on the robot

is : $F_{rep} = \sum_{i=0}^{n} F_{repi}$. So the formula for the combined force is:

$$F_{joint} = F_{att} + \sum_{i=0}^{n} F_{repi} \tag{3}$$

Although the APF is simple in structure and convenient for real-time control, it has some shortcomings.

(1).Since the gravity function is inversely proportional to the distance between the robot and the obstacle, the farther the robot is from the target point, the greater the gravity it receives. When the robot moves away from the target point, the gravity exerted on the robot will be too high, causing the robot to hit the obstacle.

(2).Due to the limitations of the APF, it is prone to local oscillation in more complex situations. The typical situation is three points and one line of robot,as shown in Fig 2. When the repulsive force and gravity are equal and the direction is opposite, the robot will fall into local oscillation and cannot escape. In addition, when the robot is trapped in a semi-closed obstacle, the APF is also unable to jump out of local oscillation.

(3).When the obstacle is very close to the target point, the target point may not be reached.

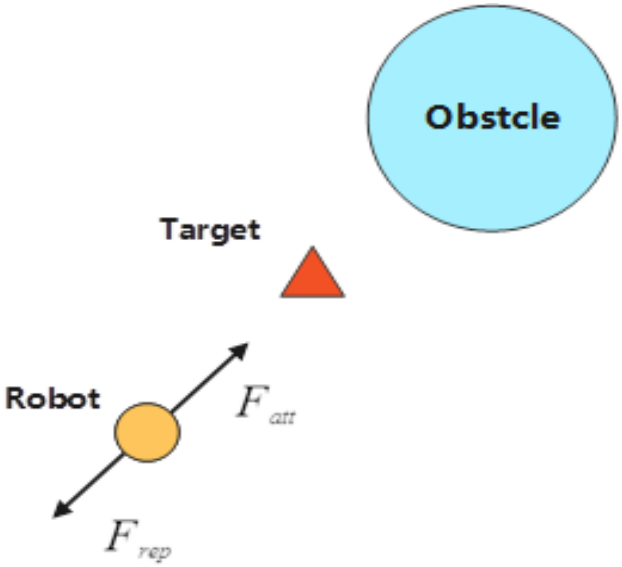

Fig. 2 Local Oscillation of the Three-point-one-Line Problem

3. Back virtual obstacle setting strategy for APF

In view of the shortcomings of APF, The algorithm redefines the traditional gravity formula, makes its path smoother, and solves the unreachable problem of the target point. In addition, for the general three-point collinear problem, this paper proposes the tangent algorithm, which can make the robot jump out of the local oscillation smoothly and reach the target point. Then for complex obstacles or even semi-closed obstacles, some algorithms

can not solve this kind of problem well. The backward strategy this paper proposed is that when the robot enters the semi-closed obstacle and falls into local oscillation, it can return to the previous step of entering the semi-closedo bstacle. Then the semi-closed obstacles are completely enclosed by adding virtual obstacles, the robot avoids entering semi-closed obstacles again.

3.1. Definition of Gravitational field function of BVO-APF

For the previous gravitational formula, this paper redefines the new gravitational function $F_{att(q)}$. The gravitational function formula is as follows:

$$F_{att(q)} = \begin{cases} n \cdot \left|\log_2(\frac{1}{\rho_{(q,q_o)}+1})\right| & \text{if}\rho_{(q,q_o)} \leq \rho_1 \\ m \cdot \left|\log_k(\rho_{(q,q_o)}+1)\right| & \text{if}\rho_{(q,q_o)} \geq \rho_1 \end{cases} \tag{4}$$

where $\rho_{(q,q_o)}$ is the distance between the robot and the target, and its mathematical expression is $\rho_{(q,q_o)} = \sqrt{(x-x_o)^2+(y-y_o)^2}$, (x, y) is the real-time coordinate position of the robot, (x_o, y_o) represents the coordinate position of the target point, ρ_1 represents a limit distance between the robot and the target point. n, $k(k > 1)$ and m are adaptive parameters, the value of k depends on the distance between the starting point and the target point.

According to the definition of the gravitational field formula, when the robot is outside the limited distance ρ_1 the gravitational force is a single increasing function, but due to the nature of the logarithmic function, the force growth of the gravitational field is relatively smooth, and the problem of collision with obstacles due to excessive gravitational force will not occur.

When the robot enters the limited distance ρ_1, according to the formula shown in formula 4. At this time, if there are obstacles around the target point, the gravitational force overcomes the repulsive force when the robot approaches the target. In this way, the robot will eventually reach the target point.

3.2. Definition of Repulsive field function of BVO-APF

The potential field of the repulsion is $U^1_{rep}(x)$, the expression formula of U_{rep} is the same as the traditional potential field method:

$$U^1_{rep}(x) = \begin{cases} \frac{1}{2}\mu(\frac{1}{\rho_{ob}} - \frac{1}{\rho})^2 & \text{if } \rho_{ob} \leq \rho \\ 0, & \text{if } \rho_{ob} \geq \rho \end{cases} \tag{5}$$

where ρ_{ob} represents the distance between the robot and the obstacle, its mathematical formula is $\rho_{ob} = \sqrt{(x-x_{ob})^2+(y-y_{ob})^2}$, ρ represents a safe distance between the robot and the obstacle. ρ_{ob} represents the distance between the mobile robot and the obstacles, μ represents the gain coefficient of repulsive field. Outside this distance, the repulsion of the obstacle has no effect on the robot. When it is less than this threshold, the repulsion of the obstacle to the robot is affected by the distance between the two.

3.3. Introduction to TAPF

For the APF, the core problem is local oscillation. This paper uses the Tangent Artificial Potential Field (TAPF)[25] to solve the three-point-one-line problem in ordinary situations. When the obstacle blocks the robot, the center point of the robot and the boundary of the obstacle model are connected. As shown in Fig 3, the pointcut provides an escape force $U^2_{rep}(x)$, the resultant force of the tangential force $U^2_{rep}(x)$ and the repulsion force $U^1_{rep}(x)$ of the obstacle to the robot provides an escape force, so the robot can smoothly jump out of the local most oscillation point.

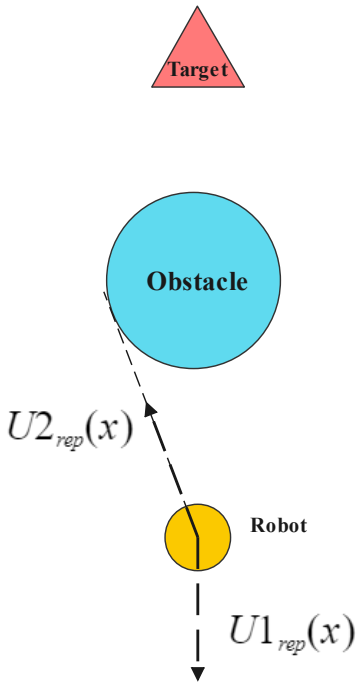

Fig. 3 Local Oscillation of the Three-point-one-Line Problem

The obstacles mentioned in this article are all approximated as a circle, and the coordinates of the obstacles are (x_{ob}, y_{ob}) and the radius of the obstacles is R. The following is the specific calculation formula:

$$\begin{cases} x_o = x_{min} + R \\ y_o = y_{min} + R \\ R = \sqrt{[(x_{max} - x_{min})/2]^2 + (y_{max} - y_{min})/2]^2} \end{cases} \tag{6}$$

where x_{max} ,x_{min} and y_{max} ,y_{min} are the maximum and minimum values of the horizontal and vertical coordinates of the obstacle in the coordinates respectively.

The value range of the direction angle of the mobile robot is$[-\pi, \pi]$, which is convenient

to calculate the direction of the robot's movement. The formula is expressed as:

$$\varphi(x,y) = \begin{cases} \arctan(\frac{y}{x}) & x > 0 \\ \pi + \arctan(\frac{y}{x}) & y \geq 0, x < 0 \\ \pi + \arctan(\frac{y}{x}) & y < 0, x < 0 \\ \frac{\pi}{2} & y > 0, x = 0 \\ \frac{-\pi}{2} & y < 0, x = 0 \end{cases} \tag{7}$$

It is also mentioned in this paper that when the robot, obstacle and target point are in a straight line, local oscillation will occur. To overcome this problem, we modify the repulsive force $U^1_{rep}(x)$ by adding a new $U^2_{rep}(x)$. Make a tangent to the obstacle from the position of robot, and the new input is along the tangent direction.

The APF repulsion field formula $U^1_{rep}(x,y)$ can be expressed as:

$$U^1_{rep}(x,y) = \mu \cdot \frac{1}{\sqrt{(x_0 - x)^2 + (y_0 - y)^2} - R} \tag{8}$$

The angle ϕ^1_{rep} between the robot center point and the obstacle center point can be expressed as:

$$\phi^1_{rep} = \varphi(y_o - y, x_o - x) \tag{9}$$

According to the knowledge of geometry, there are two tangents from a point outside the circle (x,y) to a circle with a center point(x_o, y_o) and a radius of R. Although there are two tangents, we only need to select one of them. The formula for calculating the slope of the tangent is as follows:

$$k = \frac{x_o y_o + xy - xy_o - x_o y + R\sqrt{x^2 + y^2 + x_o^2 + y_o^2 - 2x_o x - 2y_o y - R^2}}{-R^2 + x_o^2 - 2x_o x + x^2} \tag{10}$$

The horizontal and vertical coordinates of the tangent point $x_1 = \frac{-ky + x_o + k^2 x + ky_o}{1+k^2}$, $y_1 = \frac{kx_o + y + k^2 y_o - kx}{1+k^2}$, and $U^2_{rep}(x,y)$ are expressed as :

$$U^2_{rep}(x,y) = \mu \cdot \frac{1}{\sqrt{(x_1 - x)^2 + (y_1 - y)^2}} \tag{11}$$

Then we can calculate the angle between the robot and the tangent to the obstacle:

$$\phi^2_{rep} = \varphi(y_1 - y, x_1 - x) \tag{12}$$

Finally, the final form of $U_{rep}(x,y)$ can be calculated as follows.

$$\begin{bmatrix} U^x_{rep}(x,y) \\ U^y_{rep}(x,y) \end{bmatrix} = \begin{bmatrix} U^1_{rep}(x,y)\cos\phi^1_{rep} \\ U^1_{rep}(x,y)\sin\phi^1_{rep} \end{bmatrix} + \begin{bmatrix} U^2_{rep}(x,y)\cos\phi^2_{rep} \\ U^2_{rep}(x,y)\sin\phi^2_{rep} \end{bmatrix} \tag{13}$$

The above situations are all aimed at the three-point collinear problem, but the actual situation is far more complex than the three-point collinear problem. Especially for semi-closed obstacles, The TAPF cannot solve this problems.

3.4. Introduction to the principle of jumping out of semi-closed obstacles by BVO-APF algorithm

The walking-along-the-wall strategy and the technique of virtual target points are two methods that have been suggested for semi-closed obstacles. Although this issue can also be resolved, the robot will take more steps as a result. So, a BVO-APF algorithm is suggested in this study. The algorithm's main idea is that the robot can return to its original path and escape the semi-closed obstacle, as shown in Figure 4. The semi-closed obstacles are sealed using the virtual obstacle technique. Now the robot is facing a totally enclosed obstacle, we can think of it as an obstacle with a large radius. The robot can then use the tangent algorithm to effectively hop out of the semi-closed obstacles.

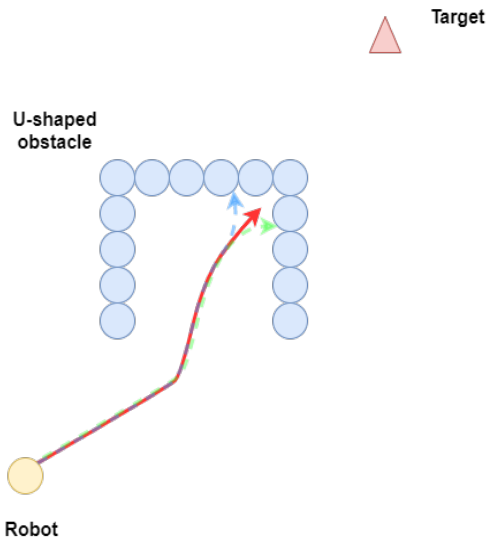

Fig. 4 Semi-closed obstacle path map

As shown in Fig.4, for the APF, it is easy for the robot to enter such a semi-closed obstacle, and the robot will inevitably fall into local oscillation. At this time, whether it is left or right, it will collide with obstacles. The TAPF and APF can not solve this problem. In the process of moving the robot forward, the algorithm judges the shape of the surrounding obstacles. When the robot enters the semi-closed obstacle, the position of the robot center point (x, y) is different from the edge obstacle of the semi-closed obstacle. There is an included angle θ between the coordinates of the two center points. When the robot does not enter the semi-closed obstacle, the angle θ is θ_+. When the robot is parallel to the center point of the most marginal obstacle, the angle θ is 0 , and when the robot enters the obstacle, the angle is θ_-.

When the mobile robot enters the semi-closed obstacle, local oscillation will occur. The mobile robot is stationary or oscillated somewhere in the semi-closed obstacle, and the mobile robot will calculate the angle θ . If it is inside the semi-closed obstacle, the mobile robot

will retreat according to the moving path when it came in. The included angle θ between the two will gradually decreases. When the included angle θ from θ_- to θ_+, it will show that the mobile robot withdraws from the obstacle.

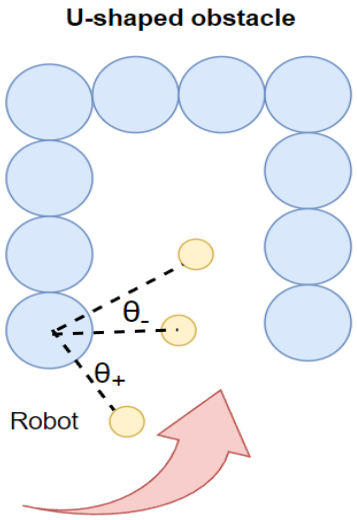

Fig. 5 The angle diagram of the mobile robot before and after entering the obstacle

In order to make the robot escape from the semi -closed obstacles smoothly, we define the included angle θ between the two center points, and the formula is as follows:

$$\theta = \begin{cases} \theta_- = -\cot(\frac{\rho_{obi}^2+\rho_{ob(i-1)}^2-\rho_i^2}{2\rho_{obi}\cdot\rho_{ob(i-1)}}) & \text{inside} \\ \theta_+ = \cot(\frac{\rho_{obi}^2+\rho_{ob(i-1)}^2-\rho_i^2}{2\rho_{obi}\cdot\rho_{ob(i-1)}}) & \text{outside} \end{cases} \tag{14}$$

where ρ_{obi} represents the distance from the current position of the mobile robot to the obstacle at the edge of the semi-closed obstacle, $\rho_{ob(i-1)}$ represents the distance between the current position of the mobile robot and the previous position of the mobile robot.The expressions are as follows:

$$\rho_{obi} = \sqrt{(x - x_{ob})^2 + (y - y_{ob})^2} \tag{15}$$

$$\rho_{ob(i-1)} = \sqrt{(x_{i-1} - x_{ob})^2 + (y_{i-1} - y_{ob})^2} \tag{16}$$

where (x_{ob}, y_{ob}) represents the coordinates of the center point of the edge obstacle, (x_{i-1}, y_{i-1}) is the position of the previous step of the mobile robot. At this time, the robot judges the included angle θ between the mobile robot and the edge obstacle. If θ is less than 0, it is deemed that the obstacle has not been withdrawn; if the included angle θ is greater than 0, it is deemed that the obstacle has been withdrawn.

When the mobile robot completely withdraws from the semi-closed obstacle, it will search the position of two edge obstacles, and the system will seal the semi-closed obstacle by adding virtual obstacles. Then jump out of the whole obstacle by using the tangent algorithm.

Generally, if the radius of the obstacle is large, the included angle θ is greater than 0, but the mobile robot does not completely jump out of the semi-closed obstacle.

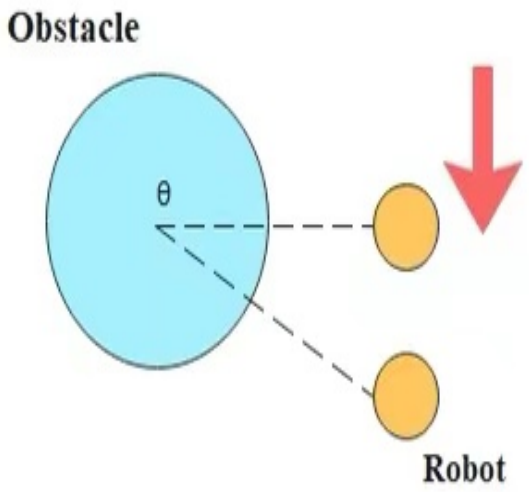

Fig. 6 Obstacles with large radius

As shown in Fig 6, in some obstacles with large radius, although the above conditions are met, the mobile robot still does not fully jump out, so we change the judgment condition of θ to θ_1 , the formula of θ_1 is as follows:

$$\theta_1 = \theta_+ + N \cdot R\delta \tag{17}$$

where δ is the angle of adjustment, R is the radius of the edge obstacle and N is the adaptive adjustment parameter. When the radius of the edge obstacle is larger, the judgment threshold of θ will increase, which will ensure that the mobile robot can completely withdraw from the obstacle. When θ is greater than 0 and θ is greater than θ_1, it is defined as the mobile robot jumping out of a semi closed obstacle.

3.5. BOV-APF algorithm flow chart

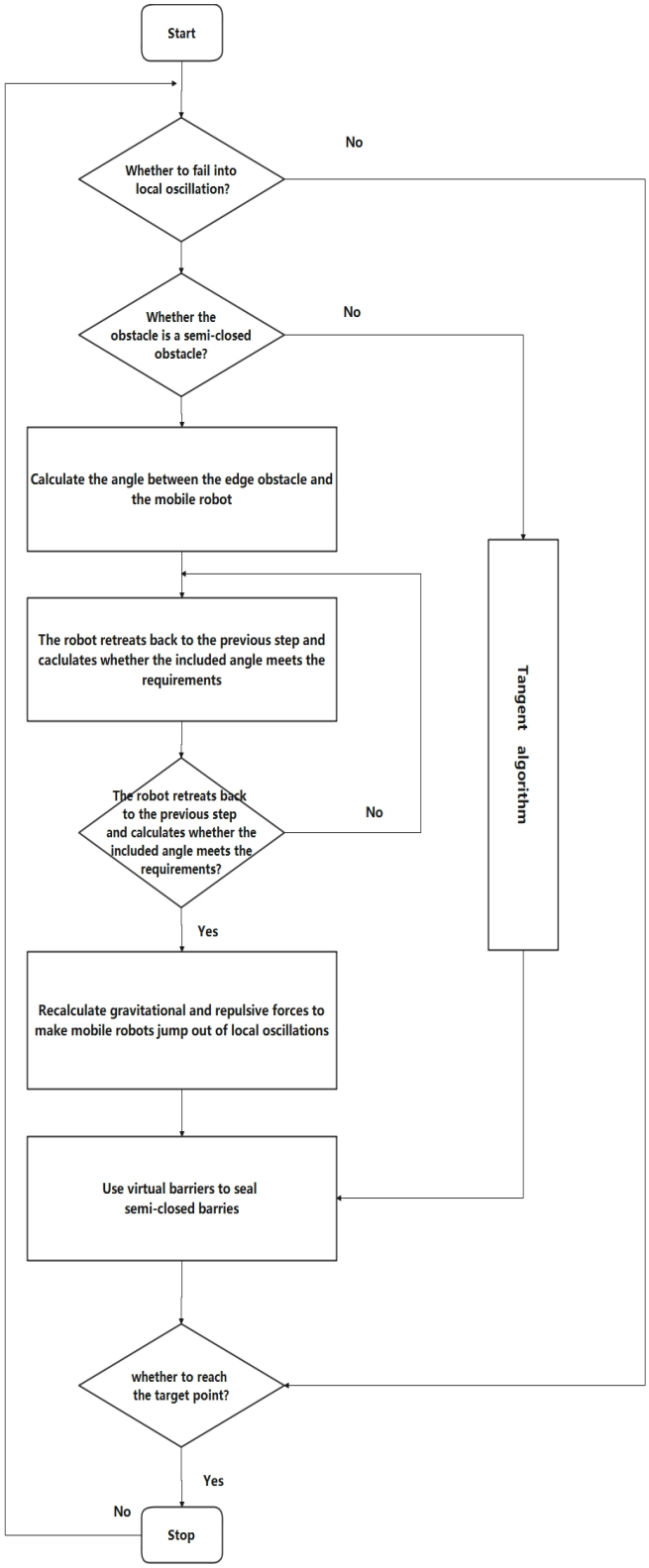

Fig. 7 BOV-APF algorithm flow chart

4. Algorithm simulation and result analysis

4.1. For the target point unreachable problem

As shown in Fig8, Fig9 and Fig10, the experiment sets the starting point position of each algorithm as (0, 0) and the target point position (44, 55). The APF algorithm and the TAPF are trapped in local oscillation at (44.3, 55.4) (44.3, 55.3) respectively. Reaching the target point, this is also the limitation of the gravitational and repulsive force functions of the traditional algorithm itself, that is, the force gradually decreases when the gravitational force approaches the target point, the repulsive force increases gradually. The gravity function of the BOV-APF algorithm will overcomes the repulsion force, and reaches the target point smoothly (44, 55).

Table 1 the table of problem 1

Algorithm	APF	TAPF	BVO-APF
Starting point	(0,0)	(0,0)	(0,0)
Target	(44,55)	(44,55)	(44,55)
Stop point	(44.3,55.4)	(44.3,55.3)	(44,55)
Obstacle coordinates	(42,52)	(42,52)	(42,52)
Situation	Failure	Failure	Success

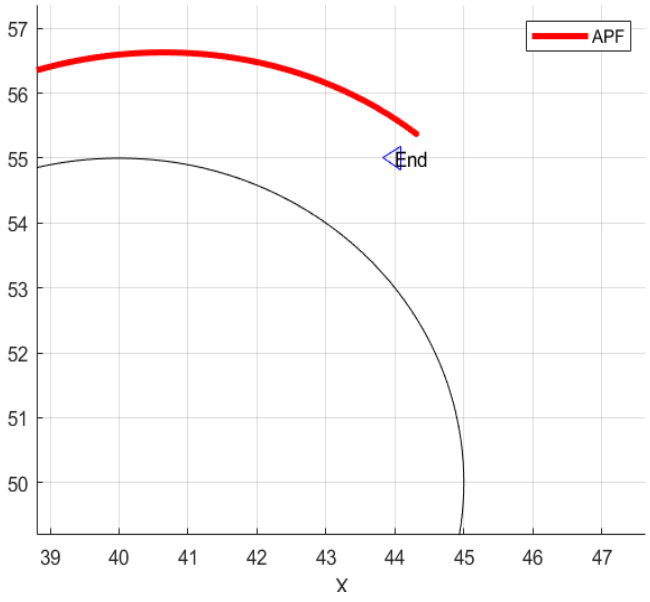

Fig. 8 Experimental diagram of traditional APF

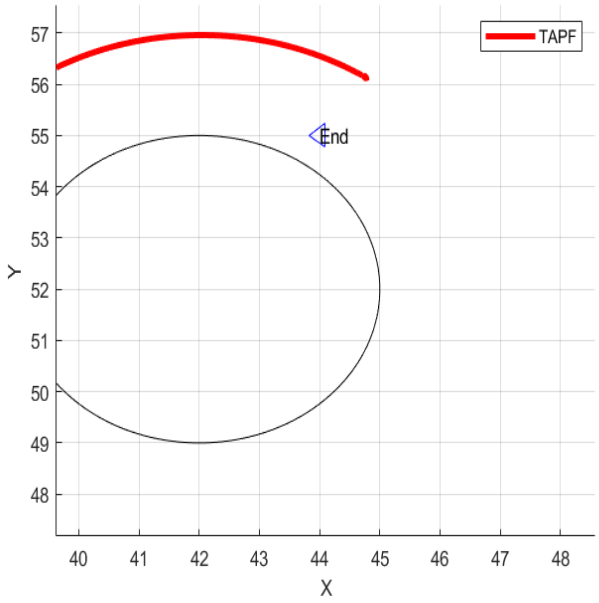

Fig. 9 Experimental diagram of traditional TAPF

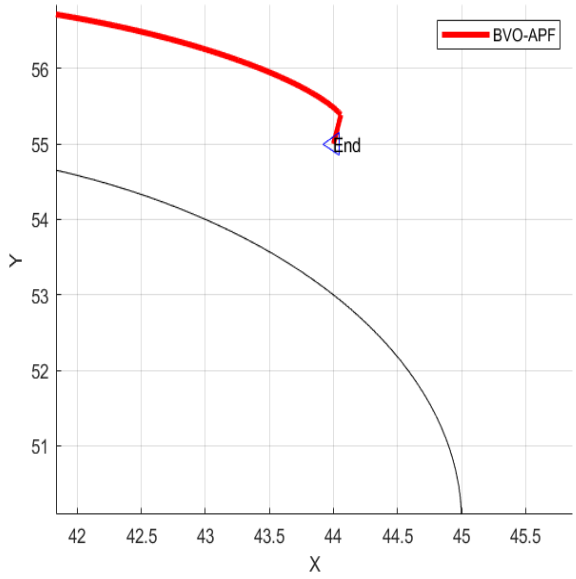

Fig. 10 Experimental diagram of traditional BVO-APF

4.2. local oscillation problem

4.2.1. Triangular semi-closed obstacle

The figure below shows the global path under different algorithms when the mobile robot faces a triangular semi-closed obstacle. From the experimental results, we can see that the APF and the TAPF cannot jump out of the local oscillation for triangular semi-closed obstacles, but the BVO-APF algorithm can solve this problem very well.

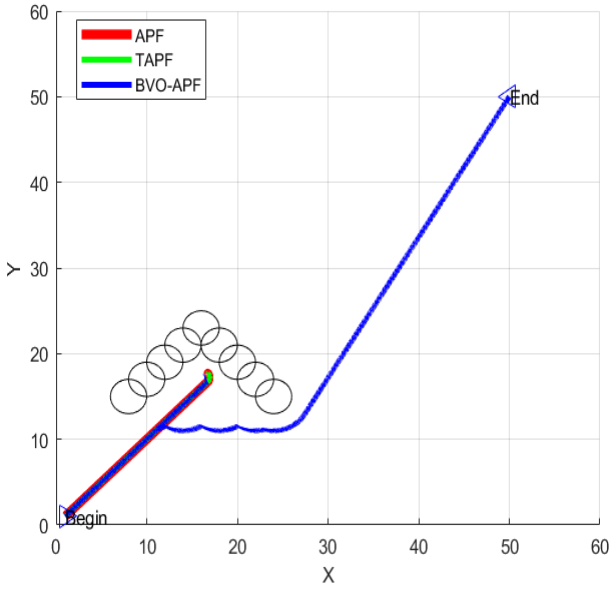

Fig. 11 Path comparison of three algorithms in triangle obstacle

4.2.2. U-shaped semi-closed obstacle

In order to verify the reliability of the BVO-APF algorithm, we tried different shapes of semi-closed obstacles to test the BVO-APF algorithm. The experimental results show that the BVO-APF algorithm can well deal with different closed obstacles.

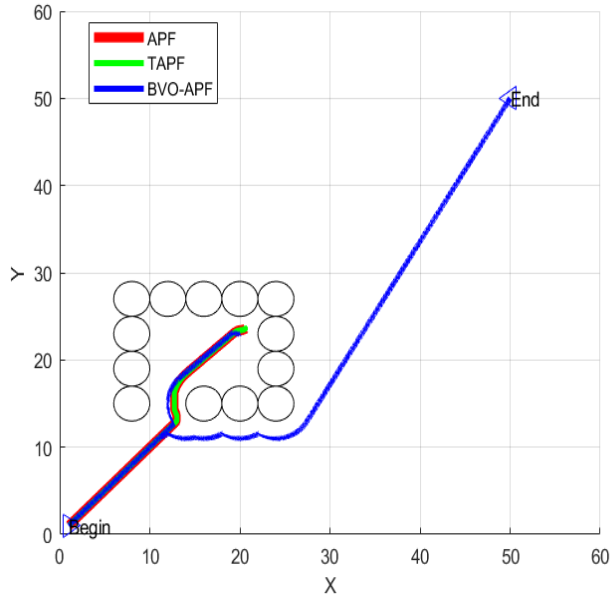

Fig. 12 Path comparison of three algorithms in U-shaped obstacles

4.3. Holistic test

To test the completeness of the BVO-APF algorithm, this paper tested the questions raised in 4.1 and 4.2 together. As shown in the experiment in the following figure, the BVO-APF algorithm can still reach the target point well when jumping out of a semi-closed obstacle (there are obstacles around the target point). However, APF and TAPF cannot jump out of closed obstacles and cannot reach the target point (there are obstacles around the target point). Figures 14-16 show the global changes in the repulsive and attractive forces for the three algorithms in Figure 13. It can be seen that both APF and TAPF are trapped in local oscillation. In the BVO-APF algorithm, the robot can reach the target point smoothly. Table 2 shows the parameters of the three global algorithms.

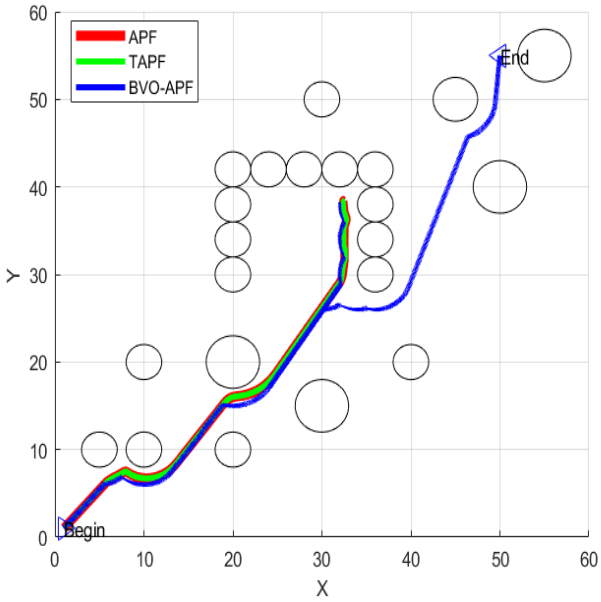

Fig. 13 Holistic Test of BVO-APF Algorithm

Table 2 the table of problem holistic test

Algorithm	APF	TAPF	BVO-APF
Starting point	(1,1)	(1,1)	(1,1)
Target	(50,55)	(50,55)	(50,55)
Stop point	(33.2,38.5)	(33.5,38.2)	(50,55)
Situation	Failure	Failure	Success
TimeUse	/	/	1.17s
Step count	61934	33119	15104

"/" indicates that the target point has not been reached

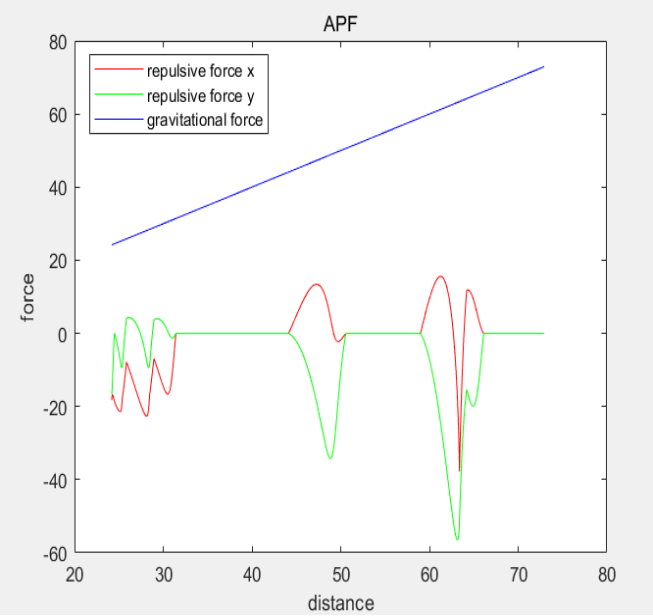

Fig. 14 APF Gravitational and repulsive force changes

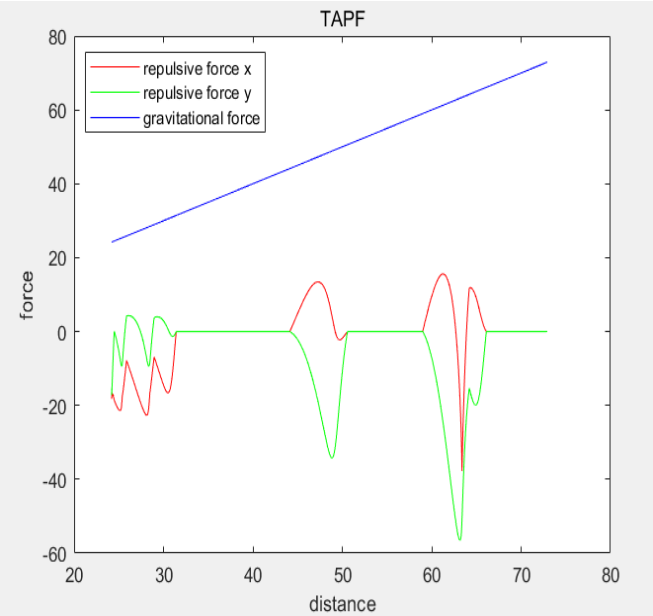

Fig. 15 TAPF Gravitational and repulsive force changes

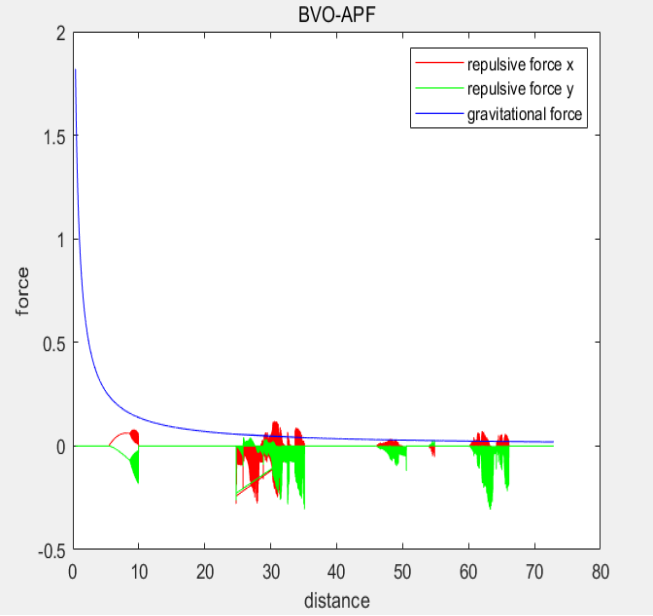

Fig. 16 BVO-APF Gravitational and repulsive force changes

4.4. ROS platform

ROS navigation system is a highly integrated functional package, which usually includes five parts: environment awareness package, self positioning package, map service package, path planning package and motion control package. During the motion of ROS robot, the environment sensor and the map server jointly build the map, and then the robot converts its position to the coordinates of the map, and sends it to the path planner through the communication mechanism. After the path planner calculates the feasible path, it sends it to the motion controller, so that the robot can move and perform tasks. Figure 17 is a complete navigation framework.

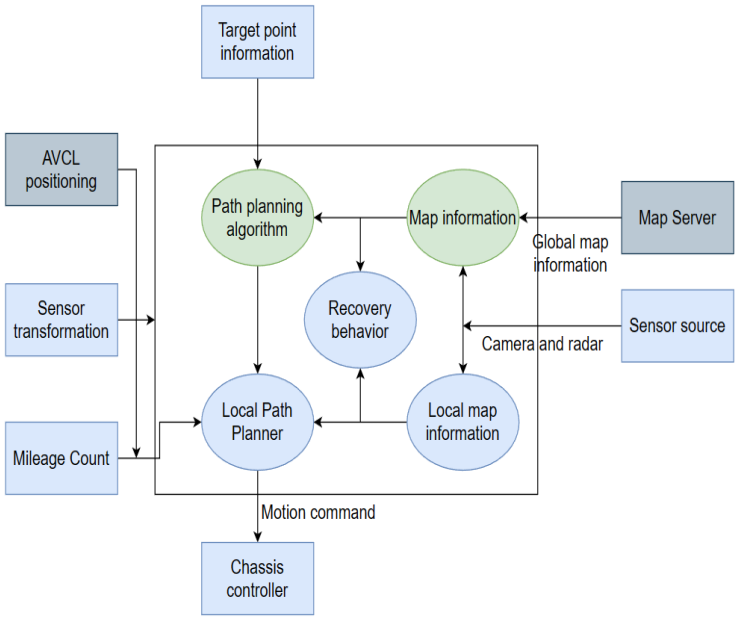

Fig. 17 ROS Navigation Framework

The environment awareness function package is mainly responsible for driving the sensor and obtaining real-time environmental information around. The sensor source is generally radar. However, with the development of depth camera, the depth camera can also obtain environmental information and calculate the depth of field to achieve the effect of radar. The odometer is mainly realized by the robot's positioning function package, which is actually composed of a series of sensors, such as using an encoder to collect the robot's linear velocity, gyroscope and accelerometer to calculate the robot's attitude, and compass to locate the robot's direction. Adaptive Monte Carlo localization is an algorithm developed during the development of robot, which can make the localization information of robot more accurate. However, this algorithm is optional, because the basic data fusion algorithm can also realize the positioning function. When the robot moves in an unknown environment, the map server can not be used. The map server will use the odometer and sensor together only when moving in a known environment. However, when these function packages implement each function, the coordinate system of each function package is different. In order to be used together, sensor coordinate conversion is required.

4.5. ROS Map establishment

This paper uses the laboratory as the background to make local and global path planning maps respectively. The physical map and physical Trolley are shown in Figure 18 and Figure 19.

Using the gmapping algorithm, and then using the keyboard to control the robot to move in the real environment, and finally build a global map. The effect of the map is shown in

Fig. 18 Local topographic map

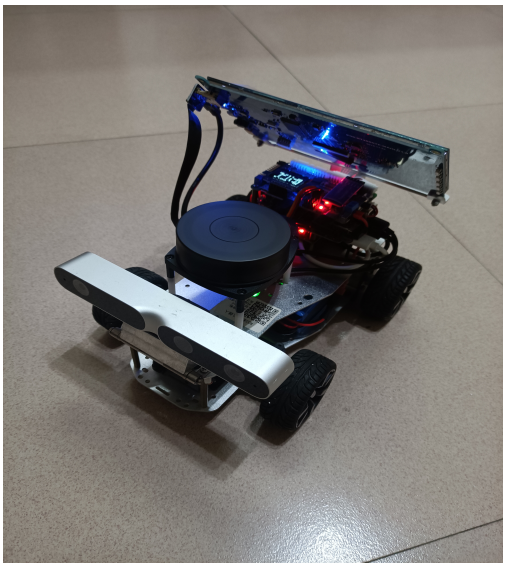

Fig. 19 Physical Drawing of ROS Trolley

Figure 20. We control the robot to generate the renderings of Figure 20 and Figure 21, and then we put the BVO-APF algorithm proposed in this paper on the robot for verification.

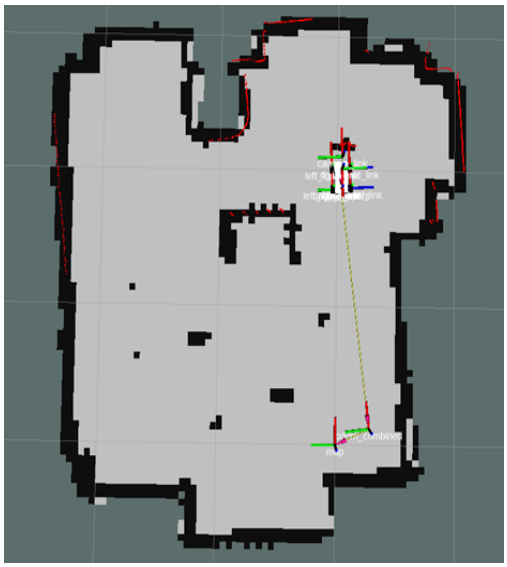

Fig. 20 Generated local path map

Fig. 21 Generated Laboratory Corridor Map

4.6. Comparison of three algorithm paths

We have made a physical comparison for the simulation experiments in paragraphs 4.2 and 4.3 of this paper. The three algorithms mentioned in this article are put into the pre scanned map. Experiments show that BVO-APF algorithm can achieve ideal results. The experimental diagram is shown in Figure 22 and Figure 23. As shown in Figure 24 and Figure 25, APF and TAPF algorithms generate local oscillations against semi enclosed

obstacles.According to the above experiments, we can see that the BVO-APF algorithm is feasible in practical application.

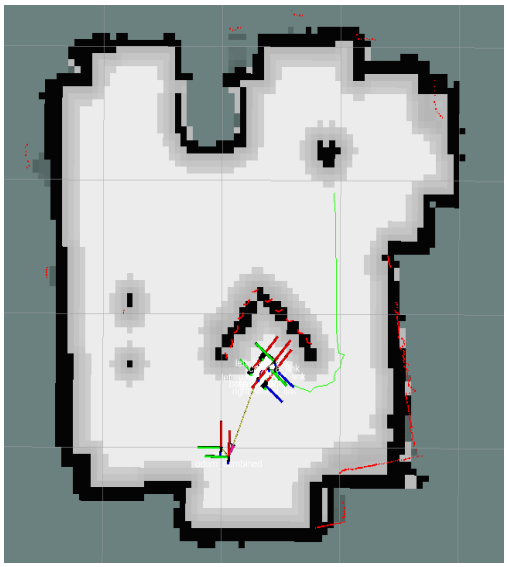

Fig. 22 Triangular obstacle path diagram for BVO-APF

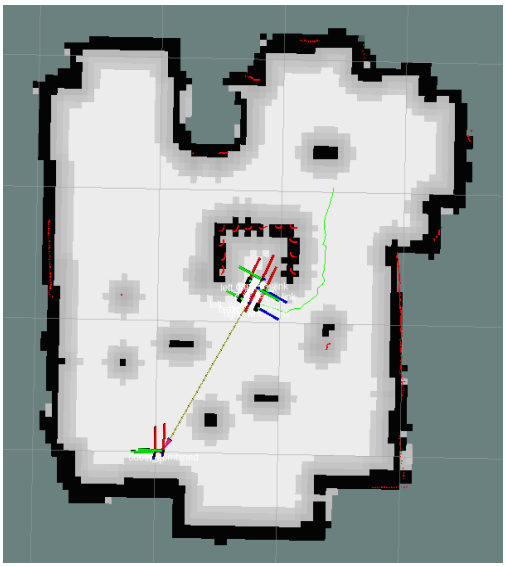

Fig. 23 Rectangle obstacle path diagram for BVO-APF

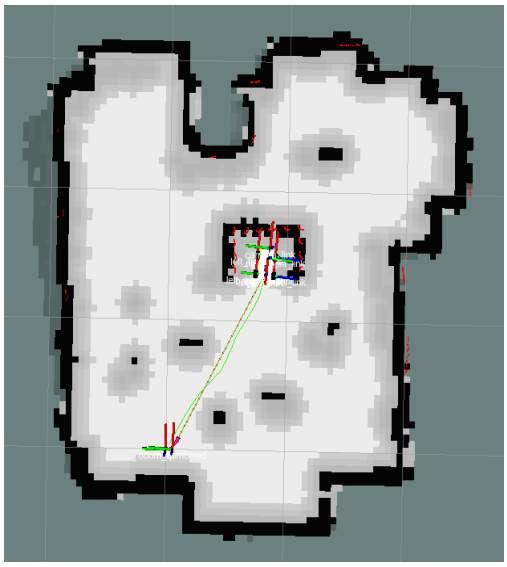

Fig. 24 Triangular obstacle path diagram for APF

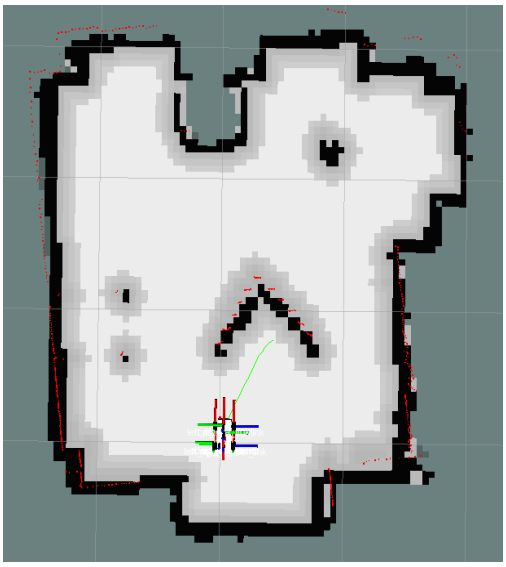

Fig. 25 Rectangle obstacle path diagram for TAPF

5. Summary

The three-point-one-line problem and the semi-closed obstacle artificial potential field method is easy to fall into the local oscillation problem. Aiming at the problem that the

target point cannot be reached, this paper proposes an improved BVO-APF. A new gravitational function is introduced to enable the robot to reach its target smoothly.

The backward virtual obstacle strategy based on tangent algorithm can make the mobile robot back to the position before entering the semi-closed obstacle. It can turn the semi-closed obstacle into a fully closed obstacle by adding virtual obstacles. The tangent strategy can use the same algorithm to jump out of an obstacle that is partially closed. Then the robot uses the tangent strategy to jump out of the semi-closed obstacle.

As future work ,the first overarching work is to apply the method in the paper to an environment with dynamic obstacles. The second task is to avoid the trolley from entering the local oscillation point as much as possible. Finally, the global path should be as short and smooth as possible while ensuring that the mobile robot can reach the target point.

6. Acknowlegdements

This research was partially funded by the National Natural Sciencce Foundation of China under grant 62073223, the National Natural Sciencce Foundation of China under grant 11502145, the China national R&D Key Research Program under grant 2020YFC227502 and the National Natural Sciencce Foundation of Shanghai under grant 22ZR1443400.

7. Reference

[1] Amador-Angulo, L., Mendoza, O., Castro, J. R., Rodríguez-Díaz, A., Melin, P., & Castillo, O. (2016). Fuzzy sets in dynamic adaptation of parameters of a bee colony optimization for controlling the trajectory of an autonomous mobile robot. *Sensors, 16*(9), 1458. doi: https://doi.org/10.3390/s16091458

[2] Chen, L., Liu, C., Shi, H., & Gao, B. (2013, September). New robot planning algorithm based on improved artificial potential field. In *2013 Third International Conference on Instrumentation, Measurement, Computer, Communication and Control* (pp. 228-232). IEEE. doi:10.1109/IMCCC.2013.55

[3] Chen, T. D., & Huang, Y. Y. (2019, May). Non-trap artificial potential field based on virtual obstacle. In *2019 IEEE 16th International Conference on Networking, Sensing and Control (ICNSC)* (pp. 275-280). IEEE.doi:10.1109/ICNSC.2019.8743340

[4] Contreras-Cruz, M. A., Ayala-Ramirez, V., & Hernandez-Belmonte, U. H. (2015). Mobile robot path planning using artificial bee colony and evolutionary programming. *Applied Soft Computing, 30,* 319-328. doi:https://doi.org/10.1016/j.asoc.2015.01.067

[5] Cheng, C., Zhu, D., Sun, B., Chu, Z., Nie, J., & Zhang, S. (2015, May). Path planning for autonomous underwater vehicle based on artificial potential field and velocity

synthesis. In *2015 IEEE 28th Canadian Conference on Electrical and Computer Engineering (CCECE)* (pp. 717-721). IEEE. doi:10.1109/CCECE.2015.7129363

[6] Dorigo, M., Di Caro, G., & Gambardella, L. M. (1999). Ant algorithms for discrete optimization. *Artificial life, 5(2)*, 137-172. doi:10.1162/106454699568728

[7] Dijkstra, E. W. (1959). A note on two problems in connexion with graphs:(Numerische Mathematik, 1 (1959), p 269-271).doi:hal-03171590, version 1

[8] Di, W., Caihong, L., Na, G., Yong, S., Tengteng, G., & Guoming, L. (2020, July). Local path planning of mobile robot based on artificial potential field. In *2020 39th Chinese Control Conference (CCC)* (pp. 3677-3682). IEEE. doi:10.23919/CCC50068.2020.9189250

[9] Fan, X., Guo, Y., Liu, H., Wei, B., & Lyu, W. (2020). Improved artificial potential field method applied for AUV path planning. *Mathematical Problems in Engineering, 2020.* doi: https://doi.org/10.1155/2020/6523158

[10] García, M. A., Montiel, O., Castillo, O., & Sepúlveda, R. (2007). Optimal path planning for autonomous mobile robot navigation using ant colony optimization and a fuzzy cost function evaluation. In *Analysis and Design of Intelligent Systems using Soft Computing Techniques* (pp. 790-798). Springer, Berlin, Heidelberg. doi:https://doi.org/10.1007/978-3-540-72432-2_79

[11] Hine, R., Willcox, S., Hine, G., & Richardson, T. (2009, October). The wave glider: A wave-powered autonomous marine vehicle. In *OCEANS 2009* (pp. 1-6). IEEE. doi:10.23919/OCEANS.2009.5422129

[12] Hou, E. S., & Zheng, D. (1994). Mobile robot path planning based on hierarchical hexagonal decomposition and artificial potential fields. *Journal of Robotic Systems, 11*(7), 605-614. doi: https://doi.org/10.1002/rob.4620110704

[13] Khatib, O. (1985, March). Real-time obstacle avoidance for manipulators and mobile robots. In *Proceedings. 1985 IEEE International Conference on Robotics and Automation* (Vol. 2, pp. 500-505). IEEE. doi:10.1109/ROBOT.1985.1087247

[14] Kamil, F., Hong, T. S., Khaksar, W., Zulkifli, N., & Ahmad, S. A. (2019). An ANFIS-based optimized Fuzzy-multilayer decision approach for a mobile robotic system in ever-changing environment. *International journal of control, Automation and Systems, 17*(1), 253-266. doi:https://doi.org/10.1007/s12555-017-0068-4

[15] Khan, A. H., Li, S., Zhou, X., Li, Y., Khan, M. U., Luo, X., & Wang, H. (2018). Neural & bio-inspired processing and robot control. *Frontiers in neurorobotics, 12*, 72. doi:https://doi.org/10.3389/fnbot.2018.00072

[16] Kabutan, R., & Nishida, T. (2018). Motion Planning by T-RRT with Potential Function for Vertical Articulated Robots. *Electrical Engineering in Japan, 204*(2), 34-43. doi: https://doi.org/10.1002/eej.23103

[17] Liu, Y., Song, R., & Bucknall, R. (2015, May). A practical path planning and navigation algorithm for an unmanned surface vehicle using the fast marching algorithm. In *OCEANS 2015-Genova* (pp. 1-7). IEEE. doi:10.1109/OCEANS-Genova.2015.7271338

[18] Lee, D., Jeong, J., Kim, Y. H., & Park, J. B. (2017, December). An improved artificial potential field method with a new point of attractive force for a mobile robot. In *2017 2nd International Conference on Robotics and Automation Engineering (ICRAE)* (pp. 63-67). IEEE. doi:10.1109/ICRAE.2017.8291354

[19] Liu,Y., Zhao, X., Xu, J., Zhu, S., & Su, D. (2022). Rapid location technology of odor sources by multi-UAV. *Journal of Field Robotics.* doi:https://doi.org/10.1002/rob.22066

[20] Montiel, O., Sepúlveda, R., & Orozco-Rosas, U. (2015). Optimal path planning generation for mobile robots using parallel evolutionary artificial potential field. *Journal of Intelligent & Robotic Systems, 79*(2), 237-257. doi:https://doi.org/10.1007/s10846-014-0124-8

[21] Rostami, S. M. H., Sangaiah, A. K., Wang, J., & Liu, X. (2019). Obstacle avoidance of mobile robots using modified artificial potential field algorithm. *EURASIP Journal on Wireless Communications and Networking, 2019(1)*, 1-19.doi:https://doi.org/10.1186/s13638-019-1396-2

[22] Roberge, V., Tarbouchi, M., & Labonté, G. (2012). Comparison of parallel genetic algorithm and particle swarm optimization for real-time UAV path planning. *IEEE Transactions on industrial informatics, 9*(1), 132-141. doi:10.1109/TII.2012.2198665

[23] Sun, Y., Fang, M., & Su, Y. (2021). AGV path planning based on improved Dijkstra algorithm. In *Journal of Physics: Conference Series* (Vol. 1746, No. 1, p. 012052). IOP Publishing. doi:10.1088/1742-6596/1746/1/012052

[24] Terano, T., Asai, K., & Sugeno, M. (1992). *Fuzzy systems theory and its applications.* Academic Press Professional, Inc.. doi:https://dl.acm.org/doi/abs/10.5555/128655

[25] Wang, D., Wang, P., Zhang, X., Guo, X., Shu, Y., & Tian, X. (2020). An obstacle avoidance strategy for the wave glider based on the improved artificial potential field and collision prediction model. *Ocean Engineering, 206*, 107356. doi:https://doi.org/10.1016/j.oceaneng.2020.107356

[26] Wu, T. (2013). Cross-country path planning based on improved ant colony algorithm. *Journal of Computer Applications, 33*(04), 1157. doi:10.3724/SP.J.1087.2013.01157

[27] Wang, Y., Chen, P., & Jin, Y. (2009, October). Trajectory planning for an unmanned ground vehicle group using augmented particle swarm optimization in a dynamic environment. In *2009 IEEE International Conference on Systems, Man and Cybernetics* (pp. 4341-4346). IEEE. doi:10.1109/ICSMC.2009.5346947

[28] XU, X., WANG, M., & MAO, Y. (2020). Path planning of mobile robot based on improved artificial potential field method. *Journal of Computer Applications, 40*(12), 3508. doi:10.11772/j.issn.1001-9081.2020050640

[29] Yingqi, X., Wei, S., Wen, Z., Jingqiao, L., Qinhui, L., & Han, S. (2021, May). A real-time dynamic path planning method combining artificial potential field method and biased target RRT algorithm. *In Journal of Physics: Conference Series* (Vol. 1905, No. 1, p. 012015). IOP Publishing. doi:10.1088/1742-6596/1905/1/012015

[30] Zhou, Y., & Huang, N. (2022). Airport AGV path optimization model based on ant colony algorithm to optimize Dijkstra algorithm in urban systems. *Sustainable Computing: Informatics and Systems*, 35, 100716. doi:https://doi.org/10.1016/j.suscom.2022.100716